

AIM2 inhibits colorectal cancer cell proliferation and migration through suppression of Gli1

Menglin Xu¹, Junfeng Wang², Haoran Li², Zhengrong Zhang², Zhengwu Cheng²

¹Department of Oncology, The First Affiliated Hospital of Wannan Medical College, Wuhu 241000, China

²Department of Gastrointestinal Surgery, The First Affiliated Hospital of Wannan Medical College, Wuhu 241000, China

Correspondence to: Zhengwu Cheng; **email:** chengzhengwu@yjsy.com

Keywords: AIM2, proliferation, migration, Gli1, colorectal cancer

Received: June 30, 2020

Accepted: September 29, 2020

Published: December 3, 2020

Copyright: © 2020 Xu et al. This is an open access article distributed under the terms of the [Creative Commons Attribution License](https://creativecommons.org/licenses/by/3.0/) (CC BY 3.0), which permits unrestricted use, distribution, and reproduction in any medium, provided the original author and source are credited.

ABSTRACT

Colorectal cancer (CRC) is a common malignant tumor and is one of the leading causes of cancer-related deaths worldwide. Absent in melanoma 2 (AIM2), as a member of the pyrin-HIN family proteins, plays contentious roles in different types of cancers. In the present work, we provide evidence that AIM2 was commonly downregulated in human CRC and loss of AIM2 significantly correlated with tumor size, depth of invasion, lymph node metastasis (LNM) and TNM (Tumor, Node, Metastases) stage in patients suffering from CRC. AIM2 knockdown promoted CRC cell proliferation, migration and epithelial-mesenchymal transition (EMT) progress, whereas AIM2 overexpression did the opposite. AIM2 inhibited glioma-associated oncogene-1 (Gli1) expression through Smoothed homolog (SMO)-independent pathway and regulated CRC cell proliferation and migration in a Gli1-dependent manner. Moreover, AIM2 could modulate Protein kinase B (AKT)/mechanistic target of rapamycin (mTOR) signaling pathway and the increased Gli1 expression and EMT progress induced by AIM2 depletion was reversed after incubation with AKT inhibitor Ly294002 in CRC cells. In conclusion, our results define AIM2 as a novel regulator of Gli1 in CRC cell growth and metastasis, and suggest that the AIM2/AKT/mTOR/Gli1 signaling axis may serve as a potential target for treatment of CRC.

INTRODUCTION

Colorectal cancer (CRC) is a common malignant tumor and is one of the leading causes of cancer-related deaths worldwide [1, 2], with annually rising incidence rates and high mortality [3]. CRC patients diagnosed at early stage have a favorable prognosis, with a 5-year survival rate of 70% to 90% [4]. Unfortunately, some CRC patients are diagnosed at advanced or metastatic stages, with a low 5-year survival rate [5]. Therefore, it is of great clinical importance to identify novel targets and to establish timely and appropriate treatment to prevent CRC progression.

Absent in melanoma 2 (AIM2), as a member of the pyrin-HIN family proteins, was originally isolated from healthy melanocytes [6]. AIM2 senses cytosolic double-stranded DNA (dsDNA) and binds to its inflammasome adaptor, apoptosis-associated speck-like protein containing a carboxy-terminal CARD (ASC), to activate the inflammasome [7, 8]. In addition to its role in inflammasome activation, AIM2 has recently been described as both a oncogene and tumor suppressor in different types of cancers. In oral squamous cell carcinoma (OSCC), AIM2 was overexpressed and ectopic AIM2 expression enhanced OSCC cell proliferation and prevented cell apoptosis [9]. Furthermore, AIM2 was highly expressed in non-small

cell lung cancer, and its overexpression facilitated cell growth and predicted poor survival of patients [10, 11]. On the other hand, excessive AIM2 expression suppressed tumor growth in breast carcinoma [12]. AIM2 was also reported to be down-regulated in hepatocellular carcinoma and loss of AIM2 expression contributed to hepatocarcinoma tumorigenesis and metastasis [13, 14]. Moreover, several recent studies demonstrated that lack of AIM2 expression exhibited oncogenic properties and was closely associated with poor outcome in CRC [15–18], but the precise functional roles and underlying mechanisms of AIM2 in CRC remain to be further explored.

The Hedgehog (Hh) signaling pathway is considered to play an essential role in cancer development and progression, including CRC [19–21]. The Hh ligand, including Sonic Hedgehog (SHh), Indian Hedgehog (IHh), and Desert Hedgehog (DHh), binds to its receptor, protein patched homolog (PTCH), leading to the release of the smoothed SMO. Released SMO then activates glioma-associated oncogene 1 (Gli1) by blocking its inhibitory partner, suppressor of fused homolog (SUFU). The SMO-dependent Gli1 activation is termed as the canonical Hh pathway [22]. The Gli1 protein, as a key transcriptional factor of Hh pathway, can also be activated by protein kinase B (AKT), extracellular signal regulated kinase (ERK) and mammalian target of rapamycin (mTOR) in a SMO-independent manner, which is known as non-canonical Hh pathway [22, 23]. Although the classical Hh pathway has been well studied, how Gli1 is regulated by SMO-independent way remains elusive.

In this study, we discovered a reduced expression and anti-tumor properties of AIM2 in CRC. Moreover, our results provided new mechanistic insights into the crucial roles of AIM2 in suppressing Gli1 through regulating AKT/mTOR pathway, which reveals a possible implication for new approaches to CRC therapy.

RESULTS

AIM2 expression is significantly decreased in CRC tissues

To further explore the anti-carcinogenic roles of AIM2 in colorectal tumorigenesis, we firstly analyzed AIM2 protein expression in human CRC tissues and para-cancer normal tissues using Immunohistochemistry (IHC) analysis. IHC staining revealed that high AIM2 protein expression was seen in 59.3% (51/86) of CRC tumor samples examined, whereas 79.5% (31/39) of normal tissues showed strong AIM2 signal (Figure 1A, 1B, Supplementary Figure 1 and Table 1). The difference

was statistically significant ($P < 0.001$, Figure 1B). Further analysis showed that AIM2 level in human CRC tissues with LNM was lower than those released from LNM ($P < 0.01$, Figure 1A, 1C).

Next, we investigated the clinical relevance of AIM2 expression in 86 CRC tumor tissues. Chi-square test analysis showed that reduced AIM2 in CRC was significantly associated with tumor size ($P=0.024$, Table 1), depth of invasion ($P=0.011$, Table 1), LNM ($P=0.001$, Table 1) and TNM stage ($P=0.003$, Table 1). However, there was no significant correlation between AIM2 protein level and other clinicopathological factors such as age, gender and tumor location ($P > 0.05$, Table 1).

Collectively, these results suggested that AIM2 is down-regulated in the development of CRC and loss of AIM2 correlates with some unfavorable clinicopathological features of CRC patients.

AIM2 expression in CRC cell lines

We first detected the levels of AIM2 protein in five different human CRC cell lines (HCT116, CCL244, SW480, SW620 and LoVo) by Western blot analysis. Compared with the low AIM2 protein expression in HCT116 and LoVo cell lines, AIM2 levels in SW480 and SW620 were much higher (Figure 2A).

Thus, in the subsequent experiments, a lentivirus vector-based shRNA technique was used to stably knocked down AIM2 expression in SW480 and SW620 cells with relatively high endogenous AIM2 level, while plasmids encoding human AIM2 or corresponding empty vector were introduced into HCT116 and LoVo cells which express relatively low endogenous AIM2. Results from Western blot analysis showed that AIM2 protein level was significantly lower in SW480 and SW620 cells stably transfected with AIM2-targeting shRNA (KD) than those transfected with control-shRNA (NC) ($P < 0.01$, Figure 2B), while AIM2 protein expression was greatly increased in cells stably transfected with human AIM2 (AIM2) compared to cells transfected with empty vector (VEC) ($P < 0.01$, Figure 2C). Furthermore, we used an AIM2-specific siRNA to knock down AIM2 expression in SW620 cell line and the knockdown efficiency was confirmed by Western blot analysis (Supplementary Figure 2A).

AIM2 plays anti-carcinogenic roles in CRC

Considering AIM2 expression was greatly decreased in CRC tissues and reduced AIM2 in CRC correlated with tumor size, depth of invasion, LNM and TNM stage, we thus examined the potential oncogenic roles

of AIM2 in CRC cells. Colony formation analysis showed that AIM2 knockdown in CRC cells significantly enhanced cell proliferation ability ($P < 0.01$, Figure 3A and Supplementary Figure 2B), while ectopic AIM2 expression had the opposite effect in HCT116 cells ($P < 0.01$, Figure 3B). In light of our *in vitro* findings, we tested the function of AIM2 in colorectal tumorigenesis with a nude mouse xenograft model. HCT116 cells stably expressing AIM2 (AIM2) or empty vector (VEC) were implanted onto the subcutaneous sites of nude mice. Growth of the implanted tumors was monitored and tumor sizes were measured every 4 days (Figure 3C). Results showed that tumor weights (Figure 3D) and sizes (Figure 3E) derived from AIM2-overexpressed HCT116 cells were notably reduced compared to their negative controls, suggesting the inhibitory effect of AIM2 on colorectal tumor growth.

Next, we evaluated the effect of AIM2 on cell migration. Results from transwell assay showed that the migration ability of CRC cells was greatly enhanced when cells lacked AIM2 ($P < 0.01$, Figure 3F and Supplementary Figure 2C). Inversely, HCT116 cells stably expressing AIM2 showed a significant decrease of migratory cells as compared with their negative controls ($P < 0.01$, Figure 3G). To further explore the effect of AIM2 on tumor metastasis, we examined the protein markers of EMT progress, which is an early event in the metastasis of cancer [24, 25]. In AIM2-depleted SW480 and SW620 cells, the protein expression of epithelial marker E-cadherin was greatly decreased, while the mesenchymal marker Vimentin protein level was significantly increased (Figure 3H). On the contrary, AIM2 overexpression in HCT116 and LoVo cells markedly promoted E-cadherin expression, but inhibited Vimentin expression (Figure 3I).

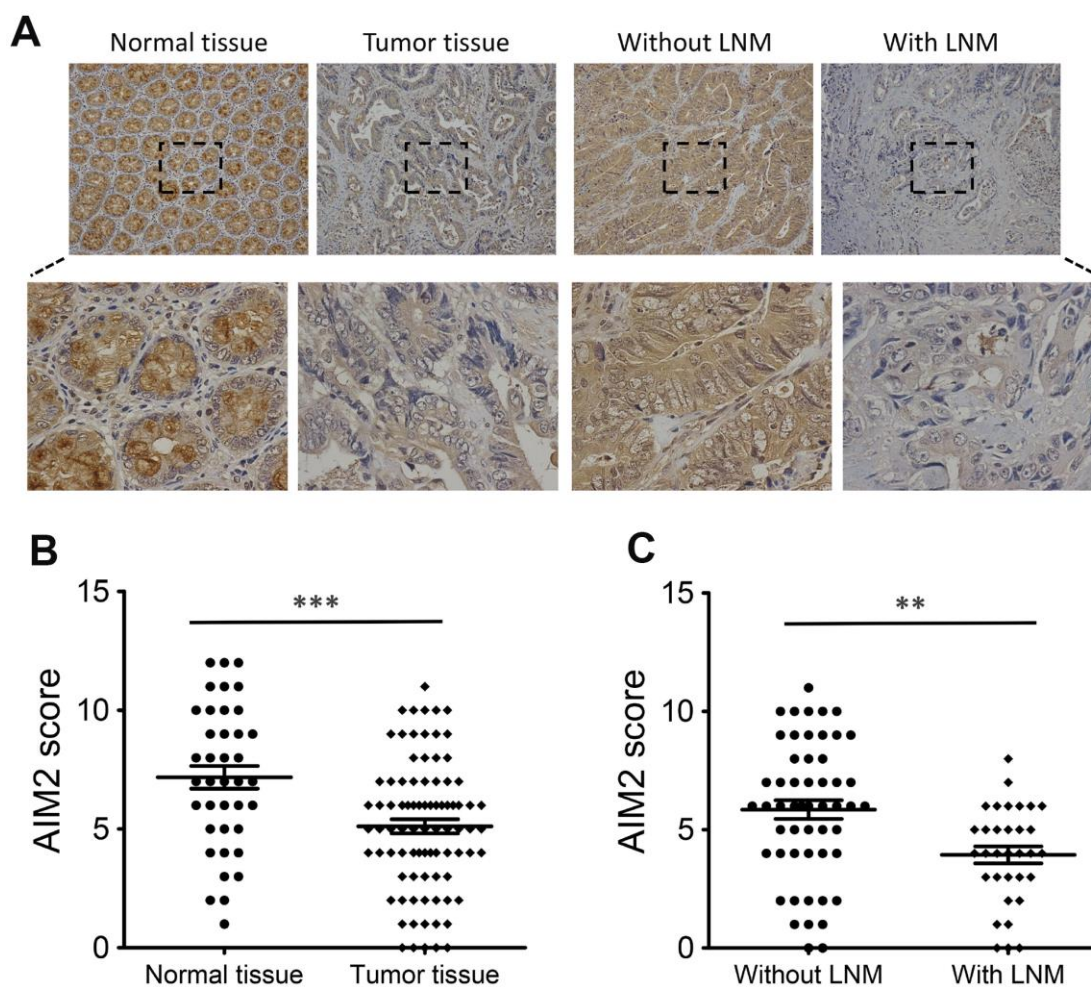


Figure 1. Expression of AIM2 protein in human CRC tissues. (A) IHC staining of AIM2 in CRC tumor tissues and surrounding normal tissues. (B) Scatter plot analysis of AIM2 IHC scores in CRC tumor tissues (n=86) and normal tissues (n=39). (C) Scatter plot analysis of AIM2 IHC scores in CRC tumor tissues with (n=31) or without LNM (n=55). ** $P < 0.01$, *** $P < 0.001$, based on a two-tailed unpaired Student's t-test.

Table 1. Correlation of AIM2 protein expression with clinic-pathological factors in 86 patients with CRC.

Clinic parameters	Total	AIM2 expression		χ^2	P value
		None or low	High		
Total	86	35 (40.7%)	51 (59.3%)		
Age (years)					
<65	35	13 (37.1%)	22 (62.9%)	0.309	0.578
>=65	51	22 (43.1%)	29 (56.9%)		
Gender					
Male	58	22 (37.9%)	36 (62.1%)	0.565	0.452
Female	28	13 (46.4%)	15 (53.6%)		
Tumor size					
<5cm	47	14 (29.8%)	33 (70.2%)	5.112	0.024*
>=5cm	39	21 (53.8%)	18 (46.2%)		
Tumor location					
Left-sided colon	28	13 (46.4%)	15 (53.6%)	0.582	0.748
Right-sided colon	27	10 (37.0%)	17 (63.0%)		
Rectum	31	12 (38.7%)	19 (61.3%)		
Depth of invasion					
T1-2	16	2 (12.5%)	14 (87.5%)	6.476	0.011*
T3-4	70	33 (47.1%)	37 (52.9%)		
Lymph node metastasis					
Yes	31	20 (64.5%)	11 (35.5%)	11.394	0.001**
No	55	15 (27.3%)	40 (72.7%)		
TNM stage					
I	13	0 (0%)	13 (100.0%)	13.699	0.003**
II	39	15 (38.5%)	24 (61.5%)		
III	32	19 (59.4%)	13 (40.6%)		
IV	2	1 (50.0%)	1 (50.0%)		

AIM2 inhibits Gli1 expression through SMO-independent pathway in CRC

Numerous studies have demonstrated that aberrant Gli1 expression in Hedgehog pathway plays a critical role in the development of CRC [20, 26] and Gli1 promotes EMT in CRC cells [27, 28]. Thus, we speculated whether Gli1 is regulated by AIM2 in CRC cells. Interestingly, Gli1 protein levels were markedly increased in AIM2-depleted SW480 and SW620 cells compared to the negative control (Figure 4A). Conversely, AIM2 elevation notably impaired Gli1 protein expression in HCT116 and LoVo cells (Figure 4B). In accordance with previous studies [29, 30], elevated Gli1 protein expression occurred in HCT116 cells treated with 20 ng/mL TGF- β for 48 h (Figure 4C). Interestingly, the increased Gli1 protein expression induced by TGF- β treatment was reversed when cells overexpressed AIM2 (Figure 4C), indicating that AIM2 overexpression impaired the effect of TGF- β on Gli1 expression. In addition, AIM2 regulation of Gli1 was also examined in xenografted tumors. Results of IHC (Figure 4D) and Western blots (Figure 4E) showed a remarkably decreased expression of Gli1 protein in tumors derived

from HCT116 cells stably expressing AIM2, suggesting Gli1 may be involved in tumor growth regulated by AIM2 in CRC.

SMO, as the central signal transducer in the classical Hh pathway, activates Gli1 by blocking its inhibitory partner SUFU [22]. To investigate whether AIM2 inhibits Gli1 expression through SMO-dependent pathway, we used Western blot analysis to test SMO protein expression by AIM2 genetic manipulation in CRC cells. As shown in Figure 4A, 4B, AIM2 knockdown or overexpression had minimal effect on SMO protein level, indicating that there might be other molecules or signaling involved in the regulation of Gli1 expression by AIM2 in CRC cells.

AIM2 suppresses CRC cell proliferation and migration via regulating Gli1

To detect whether Gli1 is implicated in the regulation of AIM2 on CRC cell proliferation and migration ability, we used Gli1 specific siRNA to silence Gli1 expression in HCT116 cells with/without AIM2 overexpression. Results from colony formation assays showed that the

proliferation ability of HCT116 cells was greatly impaired when AIM2 was overexpressed ($P < 0.01$, Figure 5A), whereas there was no significant effect of AIM2 overexpression on cell proliferation property when cells lacked Gli1 ($P > 0.05$, Figure 5A). Next, we conducted transwell migration assays to evaluate the effect of AIM2 on cell migration in the absence of Gli1. As shown in Figure 5B, the migratory HCT116 cells was markedly

reduced when cells overexpressed AIM2 ($P < 0.01$), but ectopic AIM2 failed to inhibit cell migration in Gli1-silenced HCT116 cells ($P > 0.05$). Consistent with these results, forced expression of AIM2 potently enhanced E-cadherin expression but suppressed Vimentin expression (Figure 5C). However, ectopic AIM2-induced E-cadherin increases and Vimentin losses were reversed in Gli1-depleted HCT116 cells (Figure 5C).

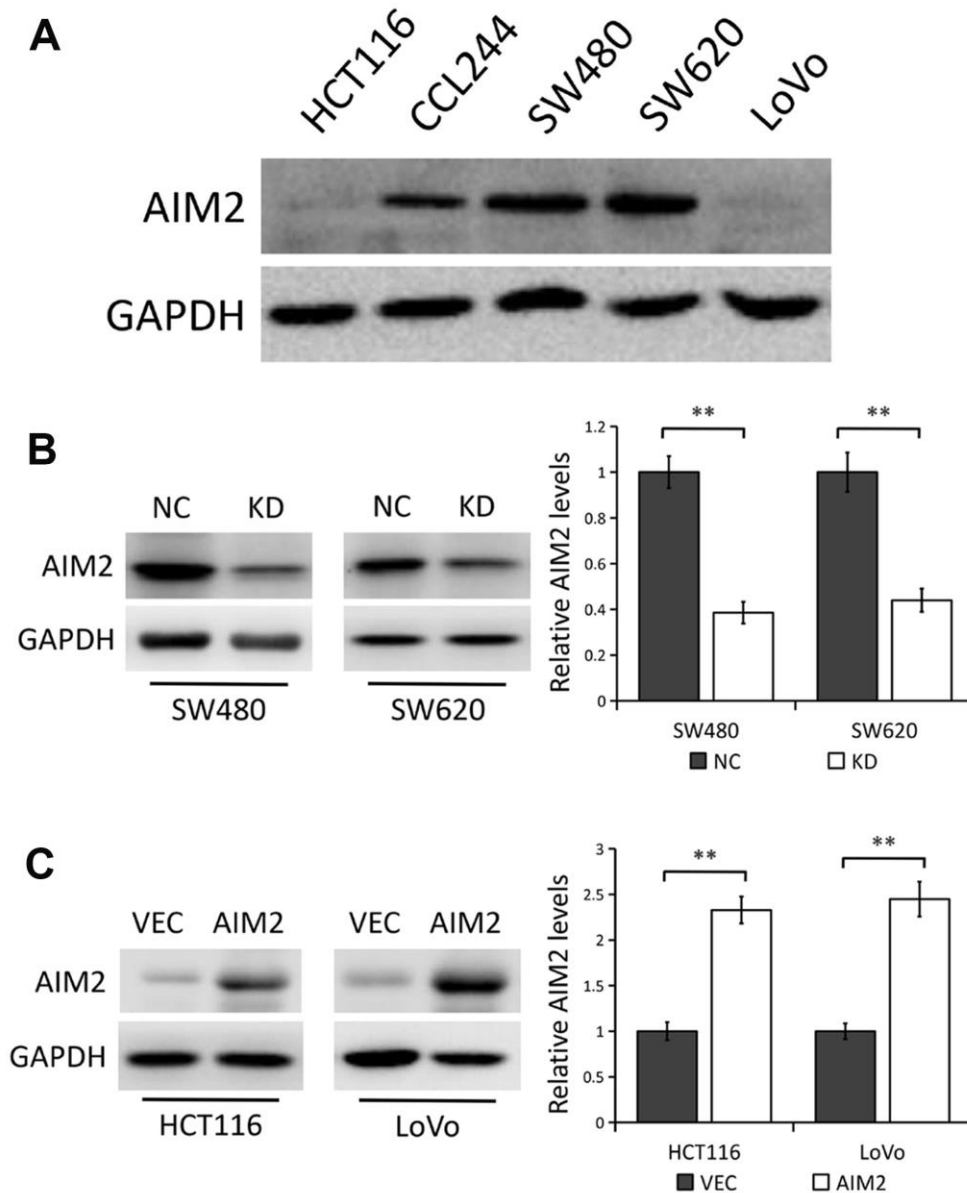


Figure 2. AIM2 protein expression in human CRC cell lines. (A) Western blots of AIM2 protein in five human CRC cell lines (HCT116, CCL244, SW480, SW620 and LoVo). GAPDH as a loading control. (B) Western blots of AIM2 protein in SW480 and SW620 cells stably transfected with control-shRNA (NC) or shRNA against AIM2 (KD). GAPDH as a loading control. Each experiment was performed at least triplicate and the bands were quantified and presented as the mean \pm SEM. (C) Western blots of AIM2 protein in HCT116 and LoVo cells stably transfected with empty vector (VEC) or plasmid encoding human AIM2 (AIM2). GAPDH as a loading control. Each experiment was performed at least triplicate and the bands were quantified and presented as the mean \pm SEM. ** $P < 0.01$, based on a two-tailed paired Student's t-test.

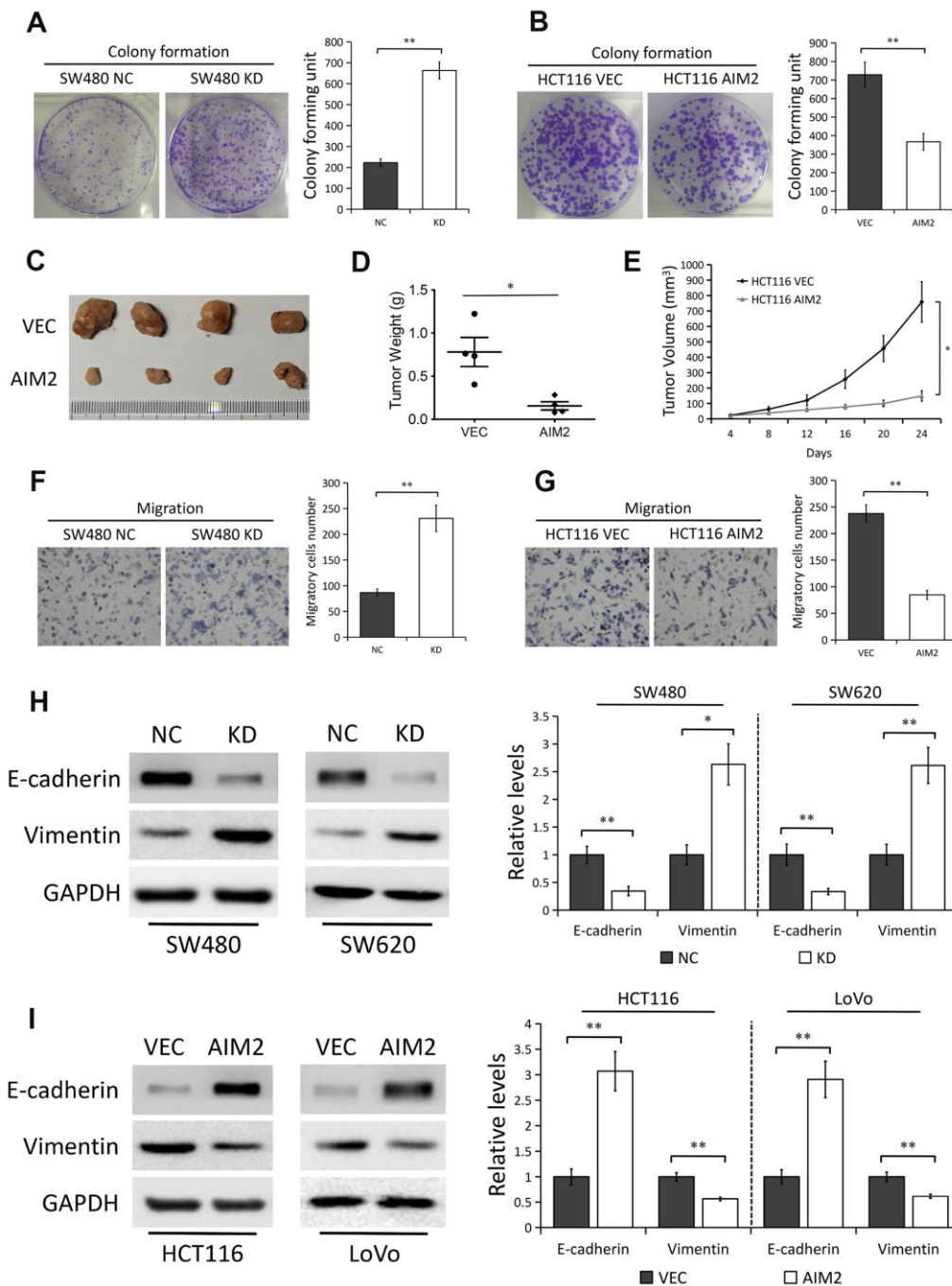


Figure 3. AIM2 plays anti-carcinogenic roles in CRC. (A) Colony formation assays to test viability of SW480 cells stably transfected with control-shRNA (NC) or shRNA against AIM2 (KD). Quantitative analysis results were presented as the mean±SEM (n=3). (B) Colony formation assays to test viability of HCT116 cells stably transfected with empty vector (VEC) or plasmid encoding human AIM2 (AIM2). Quantitative analysis results were presented as the mean±SEM (n=3). (C) Subcutaneous xenograft tumor growth in nude mice (4 per group) was measured and compared in HCT116 (VEC vs. AIM2) cell lines, and the representative image of tumors was shown. (D) Scatter plot analysis of tumor weight of each group was presented. (E) The volumes of the tumors measured every 4 days during the indicated period were shown. (F) Transwell assays to test migration ability of SW480 NC and KD cells. Quantitative analysis results were presented as the mean±SEM (n=3). (G) Transwell assays to test migration ability of HCT116 VEC and AIM2 cells. Quantitative analysis results were presented as the mean±SEM (n=3). (H) Western blots of E-cadherin and Vimentin protein in SW480 and SW620 cells stably transfected with control-shRNA (NC) or shRNA against AIM2 (KD). GAPDH as a loading control. Each experiment was performed at least triplicate and the bands were quantified and presented as the mean±SEM. (I) Western blots of E-cadherin and Vimentin protein in HCT116 and LoVo cells stably transfected with empty vector (VEC) or plasmid encoding human AIM2 (AIM2). GAPDH as a loading control. Each experiment was performed at least triplicate and the bands were quantified and presented as the mean±SEM. *P<0.05, **P<0.01, based on a two-tailed paired Student's t-test.

Furthermore, we used plasmids encoding human Gli1 to overexpress Gli1 in AIM2-overexpressed LoVo cells and the overexpression efficiency was confirmed by Western blot analysis (Figure 5D). Colony formation assays and migration assays showed that the decreased proliferation and migration ability induced by AIM2 overexpression was reversed after transfection with plasmids encoding human Gli1 (Figure 5E, 5F). Collectively, these above data suggested that AIM2 regulates CRC cell proliferation and migration in a Gli1-dependent pathway.

AIM2 regulates Gli1 expression and EMT progress through AKT/mTOR pathway

It has been reported that AIM2 regulates CRC cell viability via AKT pathway [15–17] and depletion of AIM2 expression promotes hepatocarcinoma progression

through mTOR activation [13]. Our present study suggests the possibility that other molecules or signaling might be involved in the regulation of Gli1 expression by AIM2 independent of SMO in CRC cells. Considering that an activated AKT/mTOR pathway was reported to promote Gli1 activity in a SMO-independent manner [22], we thus raised a presumption that AKT/mTOR pathway might be implicated in AIM2-induced Gli1 inhibition.

In line with previous studies [13, 15–17], we further confirmed the inhibitory effect of AIM2 on AKT/mTOR signaling pathway. As shown in Figure 6A, 6B, depleted expression of AIM2 notably increased the levels of phosphorylated AKT (p-AKT) and phosphorylated mTOR (p-mTOR) in both SW480 and SW620 cells, with no effect on their total protein levels. Conversely, Western blot analysis also identified lower phosphorylation levels of AKT and mTOR in

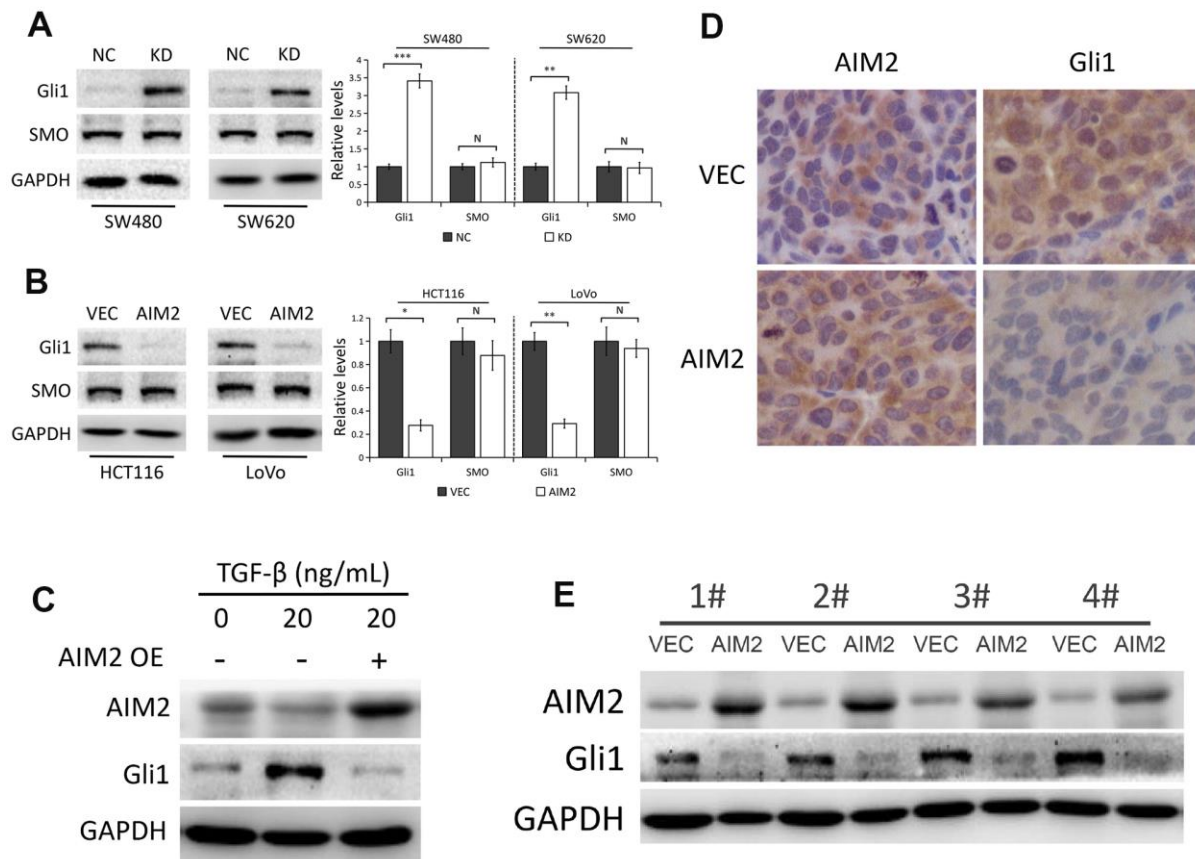


Figure 4. AIM2 inhibits Gli1 expression independent of SMO. (A) Western blots of Gli1 and SMO protein expression in SW480 and SW620 cells stably transfected with control-shRNA (NC) or shRNA against AIM2 (KD). GAPDH as a loading control. Each experiment was performed at least triplicate and the bands were quantified and presented as the mean±SEM. (B) Western blots of Gli1 and SMO protein expression in HCT116 and LoVo cells stably transfected with empty vector (VEC) or plasmid encoding human AIM2 (AIM2). GAPDH as a loading control. Each experiment was performed at least triplicate and the bands were quantified and presented as the mean±SEM. (C) Western blots of AIM2 and Gli1 protein expression in HCT116 cells treated with 20 ng/mL TGF-β for 48 h. (D) Representative images of IHC staining of AIM2 and Gli1 in subcutaneous tumors derived from HCT116 (VEC vs. AIM2) cells. (E) Western blots of AIM2 and Gli1 protein expression in subcutaneous tumors. N, nonsignificant, *P<0.05, **P<0.01, ***P<0.001, based on a two-tailed paired Student's t-test.

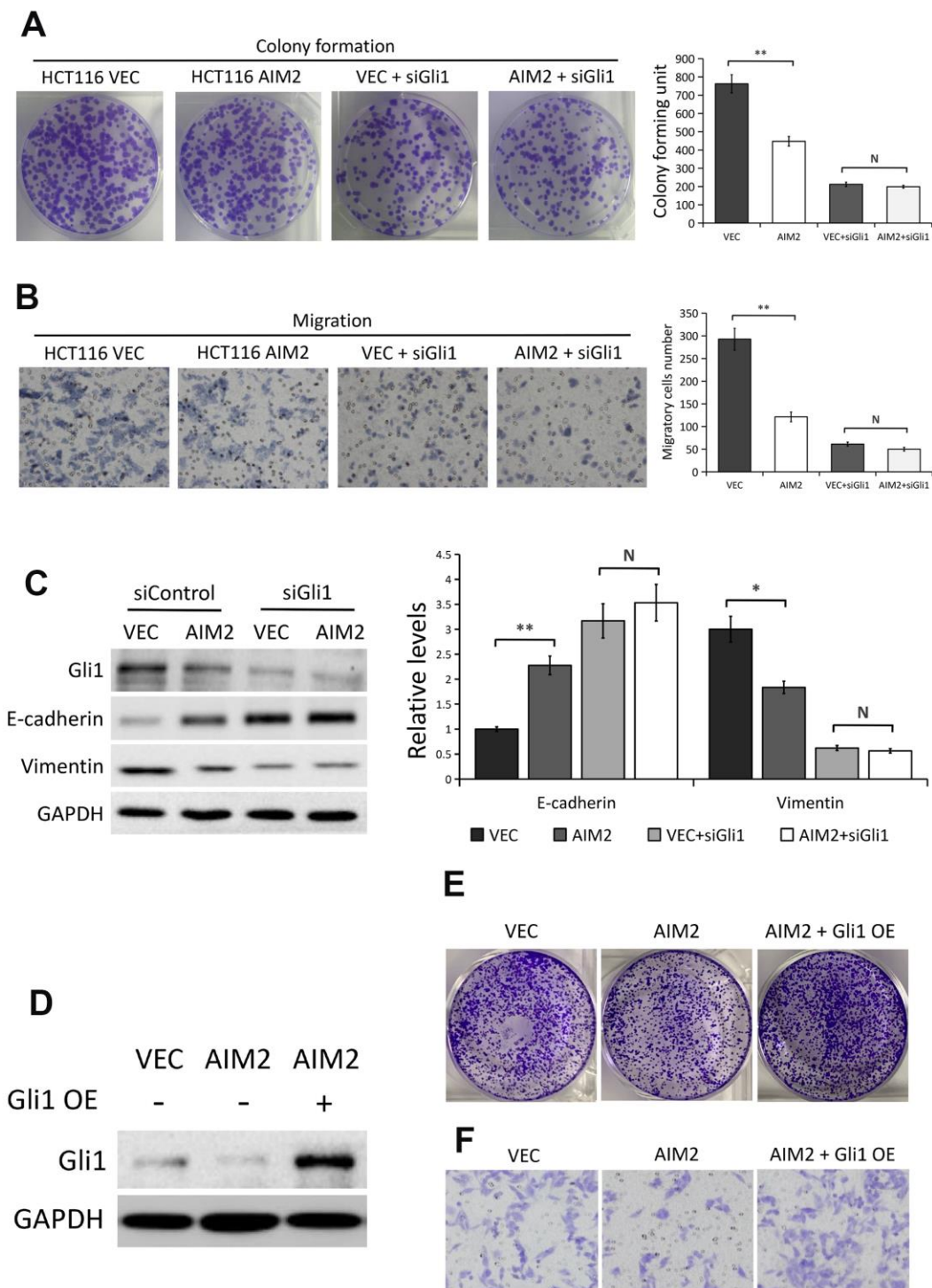


Figure 5. AIM2 inhibits HCT116 cell proliferation, migration and EMT progress in a Gli1-dependent manner. (A) Colony formation assays to test viability of HCT116 cells stably transfected with empty vector (VEC) or plasmid encoding human AIM2 (AIM2) with or without Gli1 siRNA treatment. Quantitative analysis results were presented as the mean \pm SEM (n=3). (B) Transwell assays to test migration ability of HCT116 cells stably transfected with empty vector (VEC) or plasmid encoding human AIM2 (AIM2) with or without Gli1 siRNA treatment. Quantitative analysis results were presented as the mean \pm SEM (n=3). (C) Western blots of E-cadherin and Vimentin protein expression in HCT116 cells stably transfected with empty vector (VEC) or plasmid encoding human AIM2 (AIM2) in the presence or absence of Gli1 siRNA. GAPDH as a loading control. Each experiment was performed at least triplicate and the bands were quantified and presented as the mean \pm SEM. (D) Western blots of Gli1 protein expression in LoVo (VEC vs. AIM2) cells transfected with plasmids encoding human Gli1 or empty vector. (E, F) Colony formation assay (E) and transwell assay in LoVo (VEC vs. AIM2) cells transfected with plasmids encoding human Gli1 or empty vector. N, nonsignificant, *P<0.05, **P<0.01, based on a two-tailed paired Student's t-test or ANOVA.

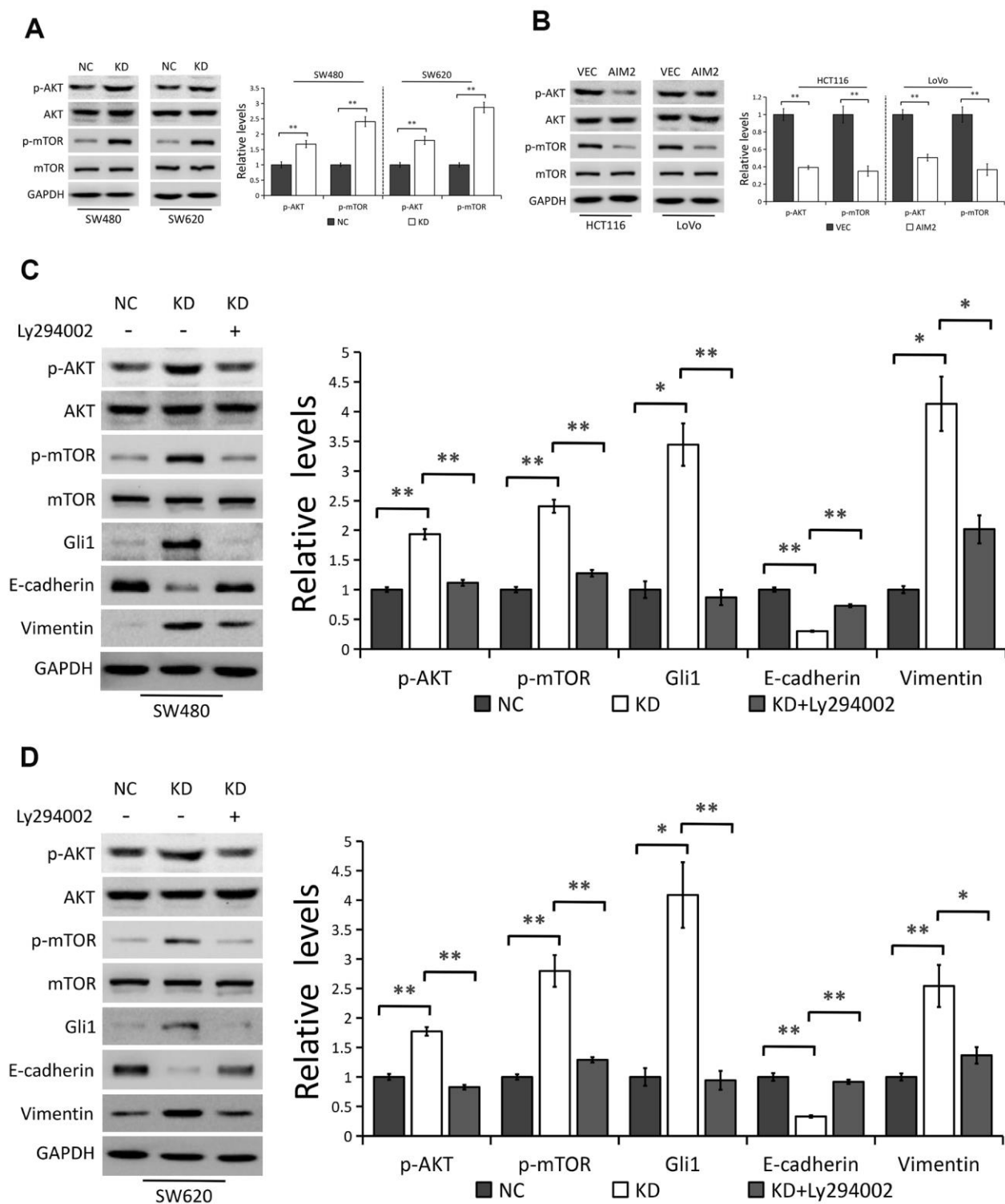


Figure 6. AIM2 regulates Gli1-mediated EMT through AKT/mTOR pathway. (A) Western blots of indicated proteins in SW480 and SW620 cells stably transfected with control-shRNA (NC) or shRNA against AIM2 (KD). GAPDH as a loading control. Each experiment was performed at least triplicate and the bands were quantified and presented as the mean±SEM. (B) Western blots of indicated proteins in HCT116 and LoVo cells stably transfected with empty vector (VEC) or plasmid encoding human AIM2 (AIM2). GAPDH as a loading control. Each experiment was performed at least triplicate and the bands were quantified and presented as the mean±SEM. (C, D) Western blots of indicated proteins in SW480 (C) and SW620 (D) cells stably transfected with control-shRNA (NC) or shRNA against AIM2 (KD) with or without Ly294002 (20 μM). GAPDH as a loading control. Each experiment was performed at least triplicate and the bands were quantified and presented as the mean±SEM. *P<0.05, **P<0.01, based on a two-tailed paired Student's t-test or ANOVA.

AIM2-overexpressed HCT116 and LoVo cells than the negative controls. We next treated AIM2-deficiency cells with Ly294002, an indirect inhibitor of AKT, to examine the role of AKT/mTOR signaling pathway in AIM2-mediated Gli1 suppression. Results showed that Ly294002 incubation remarkably suppressed AKT phosphorylation, followed by subsequent mTOR inhibition in AIM2-depleted SW480 and SW620 cells (Figure 6C, 6D). We also found that increased Gli1 protein expression induced by AIM2 knockdown was reversed in cells with Ly294002 treatment (Figure 6C, 6D), indicating the involvement of AKT/mTOR pathway in AIM2-regulated Gli1 inhibition. In addition, AIM2-deficiency-mediated EMT progress was also reversed in cells incubated with Ly294002 as evidenced by the results that Ly294002 treatment significantly increased E-cadherin expression and suppressed Vimentin expression in AIM2-depleted SW480 and SW620 cells (Figure 6C, 6D).

Collectively, our results indicated that AKT/mTOR pathway is indispensable for AIM2-regulated Gli1 inhibition and EMT progress in CRC cells.

DISCUSSION

The innate immune DNA sensor AIM2 was originally isolated from healthy melanocytes [6]. AIM2 directly binds dsDNA and initiates the recruitment of ASC and caspase-1 to activate the inflammasome [7, 8]. In cancers, the role of AIM2 is contentious and it could be either oncogenic or tumor suppressive. AIM2 protein levels were reported to be frequently overexpressed in several types of malignancies including OSCC and on-small cell lung cancer, and its overexpression promoted cancer progression and predicted poor survival of patients [9–11]. On the other hand, loss of AIM2 expression was observed in multiple tumor types including CRC [12–18]. In CRC, reduced AIM2 expression exhibited oncogenic properties and was closely associated with poor outcome [15–18]. However, the concrete molecular mechanisms of AIM2 in CRC development are elusive and remain to be further explored.

In the present work, we provide evidence that AIM2 was commonly downregulated in human CRC and was further reduced in those with LNM. Moreover, clinical data analysis showed that loss of AIM2 significantly correlated with tumor size, depth of invasion, LNM and TNM stage in patients suffering from CRC. On functional verification, our loss-of-function and gain-of-function experiments *in vitro* and *in vivo* suggested a tumor-suppressive role of AIM2 in CRC development. A published previous study [31] demonstrated that AIM2 enhanced invasion of HCT116 CRC cells, and

they also found that Vimentin mRNA expression was increased, whereas E-cadherin mRNA expression was decreased in AIM2-overexpressed HCT116 cells, which conflicts with our findings. Our results showed that AIM2 inhibited CRC cell migration and reversed EMT progress as evidenced by the fact that disruption of AIM2 inhibited E-cadherin expression and promoted Vimentin expression while AIM2 overexpression did the opposite in CRC cells, which is consistent with the previous study [17].

The Hedgehog (Hh) signaling pathway plays an essential role in cancer development and progression [19, 20]. Gli1, as a key transcriptional factor of Hh pathway, has been proposed as a candidate oncogene in CRC [20, 26, 27]. In the present study, we found that AIM2 regulated Gli1 expression in CRC cells, which is evidenced by the following observations. Our *in vitro* experiments showed that Gli1 protein levels were markedly increased in AIM2-depleted cells, but notably decreased in cells with AIM2 overexpression. In addition, AIM2 regulation of Gli1 was also examined in xenografted tumors. IHC and Western blot results showed a remarkably decreased expression of Gli1 protein in tumors derived from HCT116 cells stably expressing AIM2.

To investigate whether Gli1 is responsible for AIM2 regulation of CRC cell proliferation and migration, we silenced Gli1 in HCT116 cells with/without AIM2 overexpression. Results showed that AIM2 overexpression impaired cell proliferation and migration ability and suppressed EMT progress which was reversed by Gli1 depletion. In addition, we found that the decreased proliferation and migration ability induced by AIM2 overexpression was reversed after transfection with plasmids encoding human Gli1 (Figure 5E, 5F), which indicated the anti-carcinogenic roles of AIM2 in CRC cells is mediated by Gli1.

SMO, as the central signal transducer in the classical Hh pathway, activates Gli1 by blocking its inhibitory partner SUFU [22]. However, AIM2-induced Gli1 suppression in CRC cells is unlikely through the classical Hh pathway since SMO protein expression was not affected by AIM2 genetic manipulation, indicating that there might be other molecules or signaling involved in the regulation of Gli1 by AIM2 in CRC cells.

Previous studies showed that AIM2 regulates CRC cell viability via AKT pathway [15–17] and an activated AKT/mTOR pathway promotes Gli1 activity in a SMO-independent manner [22]. In the present work, we found that AKT/mTOR pathway is implicated in AIM2-regulated Gli1 inhibition and EMT progress in CRC cells as evidenced by the fact that AIM2 depletion

increased Gli1 protein expression and promoted EMT progress which was reversed by treatment of Ly294002, an indirect inhibitor of AKT.

In conclusion, we found that AIM2 expression was significantly decreased in CRC tissues and loss of AIM2 was strongly correlated with malignant properties of CRC cells. Mechanically, the tumor-suppressive functions of AIM2 in CRC were mediated through its participation in repressing the AKT/mTOR pathway, and the inactivated AKT/mTOR failed to increase Gli1 protein expression, resulting in the inhibition of cell proliferation and migration. This may highlight a new entry point for treating CRC by targeting the AIM2/AKT/mTOR/Gli1 signaling axis.

MATERIALS AND METHODS

CRC tissues and cell lines

Fresh and formalin-fixed tissue samples were collected from patients who underwent surgical resection in the First Affiliated Hospital of Wannan Medical College from January 2015 to January 2018. The clinicopathological features of these patients are shown in Table 1. The Institute Research Medical Ethics Committee of the First Affiliated Hospital of Wannan Medical College granted approval for this study, which was conducted in compliance with the Declaration of Helsinki. Written informed consent was obtained from all patients.

Five human CRC cell lines (HCT116, CCL244, SW480, SW620 and LoVo) were obtained from the Cell Bank of the Chinese Academy of Sciences, Shanghai, China. Cells were routinely cultured and incubated in RPMI 1640 medium (Gibco; Thermo Fisher Scientific, Inc., Waltham, MA, USA) supplemented with 10% fetal bovine serum (FBS; Gibco; Thermo Fisher Scientific, Inc., Waltham, MA, USA) and 1% penicillin/streptomycin (P/S; Gibco; Thermo Fisher Scientific, Inc., Waltham, MA, USA) at 37° C in a humidified atmosphere containing 5% CO₂.

Immunohistochemistry (IHC)

IHC staining of paraffin-embedded human or mice tumor samples were conducted according to the manufacturer's instructions. Samples were deparaffinized, rehydrated, subjected to antigen retrieval, and blocked with 3% hydrogen dioxide, followed by incubating with the primary antibodies recognizing human AIM2 (dilution 1:200; #ab93015, Abcam) or human Gli1 (dilution 1:200; #ab15179, Abcam) overnight at 4° C. Next day, the sections were incubated with secondary antibody and were visualized using a tissue staining kit (Zhongshan Biotechnology, Beijing, China). Staining intensity was

classified as 0 (lack of staining), 1 (mild staining), 2 (moderate staining) or 3 (strong staining); staining percentage was designated as 1 (<25%), 2 (25%-50%), 3 (51%-75%), or 4 (>75%). The final staining score was calculated by the multiple of color intensity and positive cell percentage, which ranged from 0 to 12. Scores 0-4 were described as none or low expression, while 5-12 as high expression.

Protein extraction and western blot analysis

Cells or tumor tissues were lysed in cold RIPA buffer (Beyotime, Beijing, China) supplemented with protease inhibitors (Roche, CA, USA) and run on SDS-PAGE gels. After transferring to the PVDF membranes, immunoblots were analyzed using the primary antibodies at 4° C overnight and were incubated with fluorescent secondary antibodies for 1 hour. Then the proteins were visualized by chemiluminescence. Antibodies used in this study were listed in Table 2.

Stable cell lines and small interfering RNA (siRNA) transfection

Lentiviral vectors plasmids were constructed by GENECHM Biotech at Shanghai, China. Transfection procedures were performed according to the manufacturer's instructions. Briefly, cells were transduced with lentiviruses for 10 h and were selected with puromycin (4 µg/ml) for 7-10 days. Transfection of siRNAs targeting human AIM2 and Gli1 was performed with Lipofectamine™ RNAiMax (Invitrogen) at a final concentration of 20 nM according to the manufacturer's instructions. The sequences specific for human AIM2 are 5'-CCCGAAGATCAACACGCTTCA-3' and 5'-GGAGAAAGUUGAUAAGCAA-3'. The sequence specific for human Gli1 5'-CUCCACAGGCAUACAGGAU-3'.

Cell viability and migration assay

For the colony formation assays, about 1,000 cells were cultivated in 6-well plates for 7-10 days. Colonies formed were washed with PBS, fixed with 4% paraformaldehyde (Beyotime, Beijing, China) and stained with 0.1% crystal violet (Beyotime, Beijing, China). Colonies containing more than 50 cells for each well were counted.

For transwell migration assays, cells were seeded into the upper chambers (Corning Incorporated, USA) in serum-free RPMI 1640 and the lower chamber was filled with RPMI 1640 containing 10% FBS. After incubation for 12-48 h, cells which had migrated through the membrane were fixed with 4% paraformaldehyde (Beyotime, Beijing, China) and stained with 0.1% crystal violet.

Table 2. Antibody information.

Name	Company	Catalog number	Dilution
AIM2	Abcam	ab93015	1:1000
p-AKT (Ser473)	Cell Signaling Technology	4058	1:1000
AKT	Cell Signaling Technology	9272	1:1000
p-mTOR	Cell Signaling Technology	9205	1:1000
mTOR	Cell Signaling Technology	2983	1:1000
E-cadherin	Cell Signaling Technology	3195	1:1000
Vimentin	Cell Signaling Technology	5741	1:1000
Gli1	Abcam	ab151796	1:1000
SMO	Abcam	ab38686	1:1000
GAPDH	Beyotime	AG019	1:1000

Subcutaneous xenograft

Nude mice (BALB/c, SPF grade, 16-18 g, 4-5 weeks and male) were purchased from Shanghai SLRC Laboratory Animal Co., Ltd. Nude mice were injected subcutaneously with 5×10^6 CRC cells. Body weight and tumor sizes were measured every 4 days. At the endpoint, tumors were harvested, weighted and stored for further analysis. All animal experimental procedures were approved by the Animal Ethics Committee of Wannan Medical College (Wuhu, China).

Statistical analysis

The results were shown as mean \pm SEM. A two-tailed Student t-test was used to compare the variables of two groups and one-way analysis of variance (ANOVA) was used for the comparison of multiple groups. Analysis of IHC results was performed by chi-square statistical test or Fisher's exact test. A P value of <0.05 was considered as significant.

AUTHOR CONTRIBUTIONS

Menglin Xu conducted the research, analyzed the data, and wrote the manuscript. Junfeng Wang, Haoran Li, Zhengrong Zhang contributed to data collection and analysis. Zhengwu Cheng designed the study and wrote the manuscript.

CONFLICTS OF INTEREST

The authors confirm that there are no conflicts of interest concerning this article.

FUNDING

This study was supported by the Nature and Science Fund from Wannan Medical College, CN (Grant Nos. WK2019F07, WK2019F09).

REFERENCES

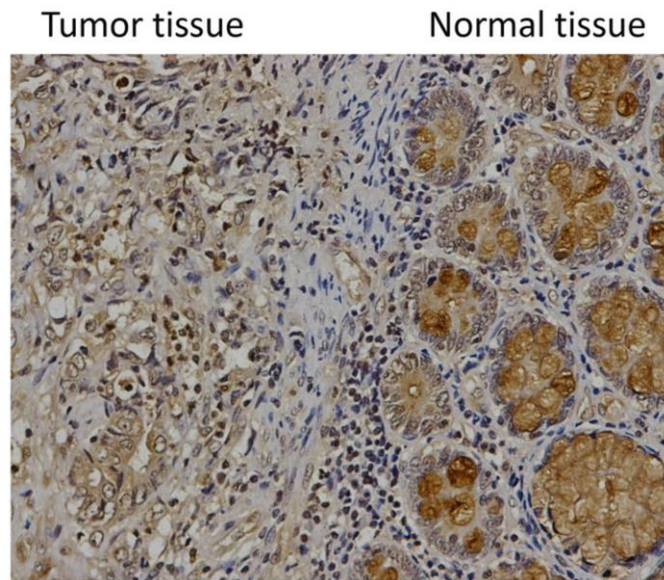
- Jacobs D, Zhu R, Luo J, Grisotti G, Heller DR, Kurbatov V, Johnson CH, Zhang Y, Khan SA. Defining early-onset colon and rectal cancers. *Front Oncol.* 2018; 8:504. <https://doi.org/10.3389/fonc.2018.00504> PMID:30460196
- Tfaily MA, Naamani D, Kassir A, Sleiman S, Ouattara M, Moacdieh MP, Jaffa MA. Awareness of colorectal cancer and attitudes towards its screening guidelines in Lebanon. *Ann Glob Health.* 2019; 85:75. <https://doi.org/10.5334/aogh.2437> PMID:31148437
- Siegel RL, Miller KD, Fedewa SA, Ahnen DJ, Meester RG, Barzi A, Jemal A. Colorectal cancer statistics, 2017. *CA Cancer J Clin.* 2017; 67:177–93. <https://doi.org/10.3322/caac.21395> PMID:28248415
- Tong GJ, Zhang GY, Liu J, Zheng ZZ, Chen Y, Niu PP, Xu XT. Comparison of the eighth version of the American joint committee on cancer manual to the seventh version for colorectal cancer: a retrospective review of our data. *World J Clin Oncol.* 2018; 9:148–61. <https://doi.org/10.5306/wjco.v9.i7.148> PMID:30425940
- Li L, Zhang L, Tian Y, Zhang T, Duan G, Liu Y, Yin Y, Hua D, Qi X, Mao Y. Serum chemokine CXCL7 as a diagnostic biomarker for colorectal cancer. *Front Oncol.* 2019; 9:921. <https://doi.org/10.3389/fonc.2019.00921> PMID:31649870
- DeYoung KL, Ray ME, Su YA, Anzick SL, Johnstone RW, Trapani JA, Meltzer PS, Trent JM. Cloning a novel member of the human interferon-inducible gene family associated with control of tumorigenicity in a model of human melanoma. *Oncogene.* 1997; 15:453–57. <https://doi.org/10.1038/sj.onc.1201206> PMID:9242382
- Hornung V, Ablasser A, Charrel-Dennis M, Bauernfeind F, Horvath G, Caffrey DR, Latz E, Fitzgerald KA. AIM2

- recognizes cytosolic dsDNA and forms a caspase-1-activating inflammasome with ASC. *Nature*. 2009; 458:514–18.
<https://doi.org/10.1038/nature07725> PMID:[19158675](https://pubmed.ncbi.nlm.nih.gov/19158675/)
8. Fernandes-Alnemri T, Yu JW, Datta P, Wu J, Alnemri ES. AIM2 activates the inflammasome and cell death in response to cytoplasmic DNA. *Nature*. 2009; 458:509–13.
<https://doi.org/10.1038/nature07710> PMID:[19158676](https://pubmed.ncbi.nlm.nih.gov/19158676/)
 9. Kondo Y, Nagai K, Nakahata S, Saito Y, Ichikawa T, Suekane A, Taki T, Iwakawa R, Enari M, Taniwaki M, Yokota J, Sakoda S, Morishita K. Overexpression of the DNA sensor proteins, absent in melanoma 2 and interferon-inducible 16, contributes to tumorigenesis of oral squamous cell carcinoma with p53 inactivation. *Cancer Sci*. 2012; 103:782–90.
<https://doi.org/10.1111/j.1349-7006.2012.02211.x> PMID:[22320325](https://pubmed.ncbi.nlm.nih.gov/22320325/)
 10. Zhang M, Jin C, Yang Y, Wang K, Zhou Y, Zhou Y, Wang R, Li T, Hu R. AIM2 promotes non-small-cell lung cancer cell growth through inflammasome-dependent pathway. *J Cell Physiol*. 2019; 234:20161–73.
<https://doi.org/10.1002/jcp.28617> PMID:[30953357](https://pubmed.ncbi.nlm.nih.gov/30953357/)
 11. Qi M, Dai D, Liu J, Li Z, Liang P, Wang Y, Cheng L, Zhan Y, An Z, Song Y, Yang Y, Yan X, Xiao H, Shao H. AIM2 promotes the development of non-small cell lung cancer by modulating mitochondrial dynamics. *Oncogene*. 2020; 39:2707–23.
<https://doi.org/10.1038/s41388-020-1176-9> PMID:[32005973](https://pubmed.ncbi.nlm.nih.gov/32005973/)
 12. Chen IF, Ou-Yang F, Hung JY, Liu JC, Wang H, Wang SC, Hou MF, Hortobagyi GN, Hung MC. AIM2 suppresses human breast cancer cell proliferation in vitro and mammary tumor growth in a mouse model. *Mol Cancer Ther*. 2006; 5:1–7.
<https://doi.org/10.1158/1535-7163.MCT-05-0310> PMID:[16432157](https://pubmed.ncbi.nlm.nih.gov/16432157/)
 13. Ma X, Guo P, Qiu Y, Mu K, Zhu L, Zhao W, Li T, Han L. Loss of AIM2 expression promotes hepatocarcinoma progression through activation of mTOR-S6K1 pathway. *Oncotarget*. 2016; 7:36185–97.
<https://doi.org/10.18632/oncotarget.9154> PMID:[27167192](https://pubmed.ncbi.nlm.nih.gov/27167192/)
 14. Chen SL, Liu LL, Lu SX, Luo RZ, Wang CH, Wang H, Cai SH, Yang X, Xie D, Zhang CZ, Yun JP. HBx-mediated decrease of AIM2 contributes to hepatocellular carcinoma metastasis. *Mol Oncol*. 2017; 11:1225–40.
<https://doi.org/10.1002/1878-0261.12090> PMID:[28580773](https://pubmed.ncbi.nlm.nih.gov/28580773/)
 15. Man SM, Zhu Q, Zhu L, Liu Z, Karki R, Malik A, Sharma D, Li L, Malireddi RK, Gurung P, Neale G, Olsen SR, Carter RA, et al. Critical role for the DNA sensor AIM2 in stem cell proliferation and cancer. *Cell*. 2015; 162:45–58.
<https://doi.org/10.1016/j.cell.2015.06.001> PMID:[26095253](https://pubmed.ncbi.nlm.nih.gov/26095253/)
 16. Wilson JE, Petrucelli AS, Chen L, Koblansky AA, Truax AD, Oyama Y, Rogers AB, Brickey WJ, Wang Y, Schneider M, Mühlbauer M, Chou WC, Barker BR, et al. Inflammasome-independent role of AIM2 in suppressing colon tumorigenesis via DNA-PK and Akt. *Nat Med*. 2015; 21:906–13.
<https://doi.org/10.1038/nm.3908> PMID:[26107252](https://pubmed.ncbi.nlm.nih.gov/26107252/)
 17. Yang Y, Zhang M, Jin C, Ding Y, Yang M, Wang R, Zhou Y, Zhou Y, Li T, Wang K, Hu R. Absent in melanoma 2 suppresses epithelial-mesenchymal transition via Akt and inflammasome pathways in human colorectal cancer cells. *J Cell Biochem*. 2019; 120:17744–56.
<https://doi.org/10.1002/jcb.29040> PMID:[31210372](https://pubmed.ncbi.nlm.nih.gov/31210372/)
 18. Dihlmann S, Tao S, Echterdiek F, Herpel E, Jansen L, Chang-Claude J, Brenner H, Hoffmeister M, Kloor M. Lack of absent in melanoma 2 (AIM2) expression in tumor cells is closely associated with poor survival in colorectal cancer patients. *Int J Cancer*. 2014; 135:2387–96.
<https://doi.org/10.1002/ijc.28891> PMID:[24729378](https://pubmed.ncbi.nlm.nih.gov/24729378/)
 19. Taipale J, Beachy PA. The hedgehog and Wnt signalling pathways in cancer. *Nature*. 2001; 411:349–54.
<https://doi.org/10.1038/35077219> PMID:[11357142](https://pubmed.ncbi.nlm.nih.gov/11357142/)
 20. Tan Y, Hu Y, Xiao Q, Tang Y, Chen H, He J, Chen L, Jiang K, Wang Z, Yuan Y, Ding K. Silencing of brain-expressed X-linked 2 (BEX2) promotes colorectal cancer metastasis through the Hedgehog signaling pathway. *Int J Biol Sci*. 2020; 16:228–38.
<https://doi.org/10.7150/ijbs.38431> PMID:[31929751](https://pubmed.ncbi.nlm.nih.gov/31929751/)
 21. Park SH, Jeong S, Kim BR, Jeong YA, Kim JL, Na YJ, Jo MJ, Yun HK, Kim DY, Kim BG, Lee DH, Oh SC. Activating CCT2 triggers Gli-1 activation during hypoxic condition in colorectal cancer. *Oncogene*. 2020; 39:136–50.
<https://doi.org/10.1038/s41388-019-0972-6> PMID:[31462707](https://pubmed.ncbi.nlm.nih.gov/31462707/)
 22. Wang Y, Ding Q, Yen CJ, Xia W, Izzo JG, Lang JY, Li CW, Hsu JL, Miller SA, Wang X, Lee DF, Hsu JM, Huo L, et al. The crosstalk of mTOR/S6K1 and hedgehog pathways. *Cancer Cell*. 2012; 21:374–87.
<https://doi.org/10.1016/j.ccr.2011.12.028> PMID:[22439934](https://pubmed.ncbi.nlm.nih.gov/22439934/)
 23. Teperino R, Aberger F, Esterbauer H, Riobo N, Pospisilik JA. Canonical and non-canonical hedgehog signalling and the control of metabolism. *Semin Cell Dev Biol*. 2014; 33:81–92.
<https://doi.org/10.1016/j.semcdb.2014.05.007> PMID:[24862854](https://pubmed.ncbi.nlm.nih.gov/24862854/)

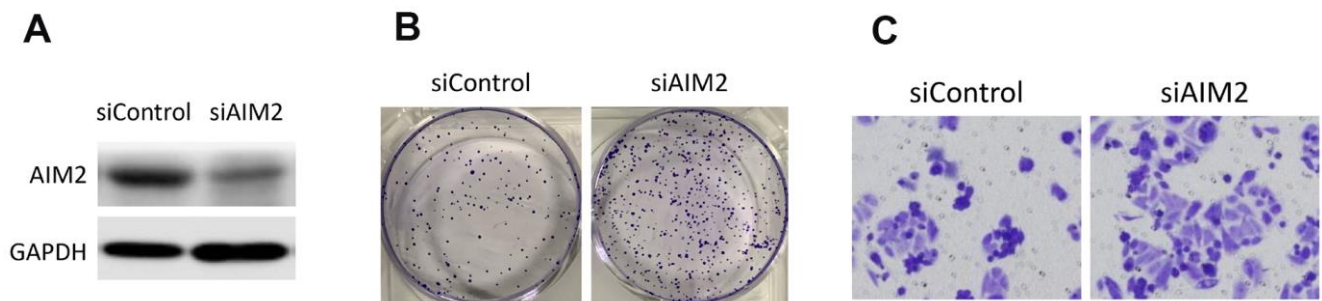
24. Gonzalez DM, Medici D. Signaling mechanisms of the epithelial-mesenchymal transition. *Sci Signal*. 2014; 7:re8.
<https://doi.org/10.1126/scisignal.2005189>
PMID:[25249658](https://pubmed.ncbi.nlm.nih.gov/25249658/)
25. Thiery JP, Acloque H, Huang RY, Nieto MA. Epithelial-mesenchymal transitions in development and disease. *Cell*. 2009; 139:871–90.
<https://doi.org/10.1016/j.cell.2009.11.007>
PMID:[19945376](https://pubmed.ncbi.nlm.nih.gov/19945376/)
26. Yang Z, Zhang C, Qi W, Cui Y, Xuan Y. GLI1 promotes cancer stemness through intracellular signaling pathway PI3K/Akt/NFκB in colorectal adenocarcinoma. *Exp Cell Res*. 2018; 373:145–54.
<https://doi.org/10.1016/j.yexcr.2018.10.006>
PMID:[30321514](https://pubmed.ncbi.nlm.nih.gov/30321514/)
27. Zhang C, Wang Y, Feng Y, Zhang Y, Ji B, Wang S, Sun Y, Zhu C, Zhang D, Sun Y. Gli1 promotes colorectal cancer metastasis in a Foxm1-dependent manner by activating EMT and PI3K-AKT signaling. *Oncotarget*. 2016; 7:86134–47.
<https://doi.org/10.18632/oncotarget.13348>
PMID:[27863385](https://pubmed.ncbi.nlm.nih.gov/27863385/)
28. Lin WF, Lin XL, Fu SW, Yang L, Tang CT, Gao YJ, Chen HY, Ge ZZ. Pseudopod-associated protein KIF20B promotes Gli1-induced epithelial-mesenchymal transition modulated by pseudopodial actin dynamic in human colorectal cancer. *Mol Carcinog*. 2018; 57:911–25.
<https://doi.org/10.1002/mc.22812> PMID:[29573464](https://pubmed.ncbi.nlm.nih.gov/29573464/)
29. Lin YT, Wu KJ. Epigenetic regulation of epithelial-mesenchymal transition: focusing on hypoxia and TGF-β signaling. *J Biomed Sci*. 2020; 27:39.
<https://doi.org/10.1186/s12929-020-00632-3>
PMID:[32114978](https://pubmed.ncbi.nlm.nih.gov/32114978/)
30. Sun SL, Wang XY. TGF-β1 promotes proliferation and invasion of hepatocellular carcinoma cell line HepG2 by activating GLI-1 signaling. *Eur Rev Med Pharmacol Sci*. 2018; 22:7688–95.
https://doi.org/10.26355/eurev_201811_16389
PMID:[30536311](https://pubmed.ncbi.nlm.nih.gov/30536311/)
31. Patsos G, Germann A, Gebert J, Dihlmann S. Restoration of absent in melanoma 2 (AIM2) induces G2/M cell cycle arrest and promotes invasion of colorectal cancer cells. *Int J Cancer*. 2010; 126:1838–49.
<https://doi.org/10.1002/ijc.24905> PMID:[19795419](https://pubmed.ncbi.nlm.nih.gov/19795419/)

SUPPLEMENTARY MATERIALS

Supplementary Figures



Supplementary Figure 1. IHC staining of AIM2 in CRC tumor tissues and surrounding normal tissues from the same slide.



Supplementary Figure 2. AIM2 plays anti-carcinogenic roles in CRC. (A) Western blots of AIM2 protein in SW620 cells transfected with control-siRNA (siControl) or siRNA against AIM2 (siAIM2). GAPDH as a loading control. (B) Colony formation assays to test proliferation ability of SW620 cells transfected with siControl or siAIM2. (C) Transwell assays to test migration ability of SW620 cells transfected with siControl or siAIM2.